Shaped Solution Domains for Snow Properties

RAE A. MELLOH,[1] SALLY A. SHOOP,[2] AND BARRY A. COUTERMARSH[2]

ABSTRACT

The objective of this work was to develop a method for distributing snow properties on a landscape that is less dependent on extensive mass and energy balance modeling, yet provides a realistic distribution of snow depth and density across the environmental gradients of elevation, slope, azimuth, and forest type. In this paper, we present important progress toward development of such an approach. A shaped solution domain was identified for snow depth, water equivalent, and density. The pinched-cone shape describes the differentiation of the snow properties with slope and azimuth and is approximated by an analytical equation with only two coefficients. Knowledge of the solution domain shape permits a few model runs or measurements to be exploited to define a continuous solution for all slope–azimuth combinations. The shaped solutions morph over time and environmental gradients.

Keywords: Shaped solution domain, Snow cone, Snow distribution, Snow properties

INTRODUCTION

This research effort arose from a requirement for distributed snow depth and density for use in high-resolution ground vehicle mobility assessment models used by the U.S. Army (Shoop et al. 2004, Richmond et al. 2005). The requirement was for a realistic distribution of snow depth and density across the environmental gradients of elevation, slope, azimuth, and forest type. An approach that is widely applicable and that decreases the dependence on extensive snow property modeling is needed because the computational and data storage aspects of the mobility model cannot be overburdened by snow process computations and snow solution storage. Yet, the distribution of snow properties across a landscape is a complex problem that requires distribution of mass and energy balance in a high-resolution (30-m) landscape.

One way to visualize this problem is to determine the likely snow depth at a remote point, given a snow depth at a point on a landscape (Fig. 1). The known point might be where we are standing, at a low elevation and on a south-facing slope. The point in question may be across the next ridge on a north-facing slope and at higher elevation. We know there is likely to be more snow at the remote point, but we do not know how much more. A method for making this extrapolation to an unknown point (or every point in the landscape) without resorting to extensive calculations would be quite useful.

[1] Correspondence to Rae A. Melloh, U.S. Army Engineer Research and Development Center, Cold Regions Research and Engineering Laboratory, 72 Lyme Road, Hanover, NH USA 03755-1290, e-mail rmelloh@crrel.usace.army.mil.

[2] U.S. Army Engineer Research and Development Center, Cold Regions Research and Engineering Laboratory, 72 Lyme Road, Hanover, NH USA 03755-1290.

In this paper, we present important progress toward development of such an approach. We have found that the solution domains for snow depth, snow water equivalent, and snow density have a predictable shape that can be approximated by an analytical equation with only two coefficients.

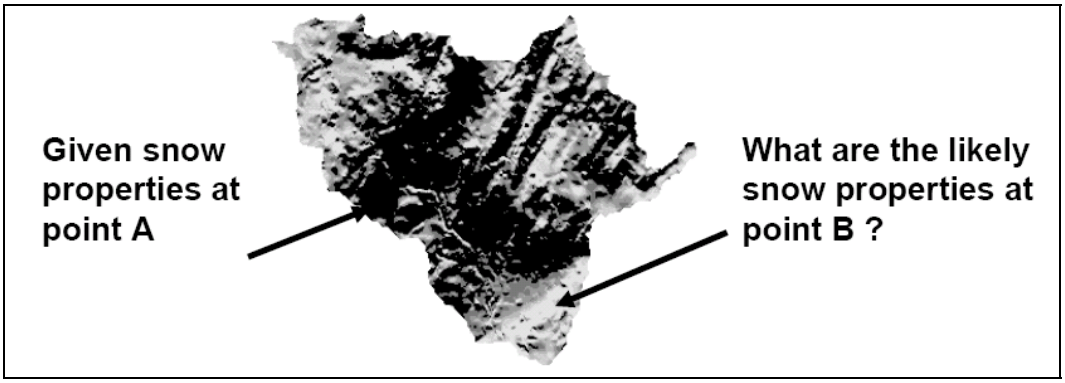

Figure 1. Snow depth across a landscape showing shallow snow (dark) at south-facing point A and deeper snow (light tone) on north-facing slope and higher elevation point B.

BACKGROUND AND APPROACH

The approach taken was to investigate snow properties as a function of slope, azimuth, elevation, and forest canopy transmissivity using a snow model that has a proven record of accurately representing snowpack processes. The model solution domain was analyzed for structure in snow property differentiation without mapping to any particular landscape. SNTHERM (Jordan 1991), SHAW (Flerchinger et al. 1994), UEB (Tarboton and Luce 1996), and ISNOBAL (Marks 1999) are examples of physically based models that accurately simulate mass and energy transfer in snowpacks. The complexity and computational intensity of the models and meteorological driver requirements usually restrict their use to point simulations or small research drainage basins (Marks 1999). With the exception of ISNOBAL, these models are not intended for explicit mapping (pixel by pixel). We chose SNTHERM (Jordan 1991) because of past experience with the model (Melloh et al. 2004) and used a recent update (SLTHERM) that includes mass and energy transfer between the snow and soil.

We designed a method that would be broadly applicable to a hilly, forested landscape in New Hampshire or Vermont similar to the landscapes of the Sleepers River Research Watershed near Danville, Vermont; Hubbard Brook Experimental Forest near Thornton, New Hampshire; and the Ethan Allen Firing Range near Jericho, Vermont. The first planned application of the method developed here is for a high-resolution mobility model of the Ethan Allen Firing Range. Hubbard Brook, Sleepers River, and Ethan Allen all have similar climate, topography, and elevation ranges from approximately 200 to 1000 m. The tree species are predominantly northern deciduous hardwoods, including sugar maple (*Acer sacharum*), beech (*Fagus grandifoia*) and yellow birch (*Betula allegheniensis*). White ash (*Fraximus americana*) is found at middle and lower elevations. Red spruce (*Picea rubens*), balsam fir (*Abies balsamea*), and white birch (*Betula papyrifera var. cordifolia*) occur at the higher elevations and on rock outcrops. Hemlock (*Tsunga canadensis*) is found along the streams.

Solar radiation, when calculated as a function of slope and azimuth and visualized in an array, displays a gradually changing symmetrical pattern across the array and with calendar progression (Fig. 2). It seemed plausible that snowmelt differentiation due to slope and azimuth would also follow a tractable pattern. Slope–azimuth combinations were selected by examining plots of clear-sky solar radiation over the snow season (Fig. 2). South- and north-facing exposures were emphasized over east- and west-facing exposures in the selection of slope–azimuth combinations because the magnitude of daily solar radiation varies less with terrain slope for east and west exposures. Modifications were made to the base meteorological data to drive the snowpack energy

and mass balances for 540 environments: the product of 27 slope–azimuth combinations, five forest canopy transmissivities, and four elevations.

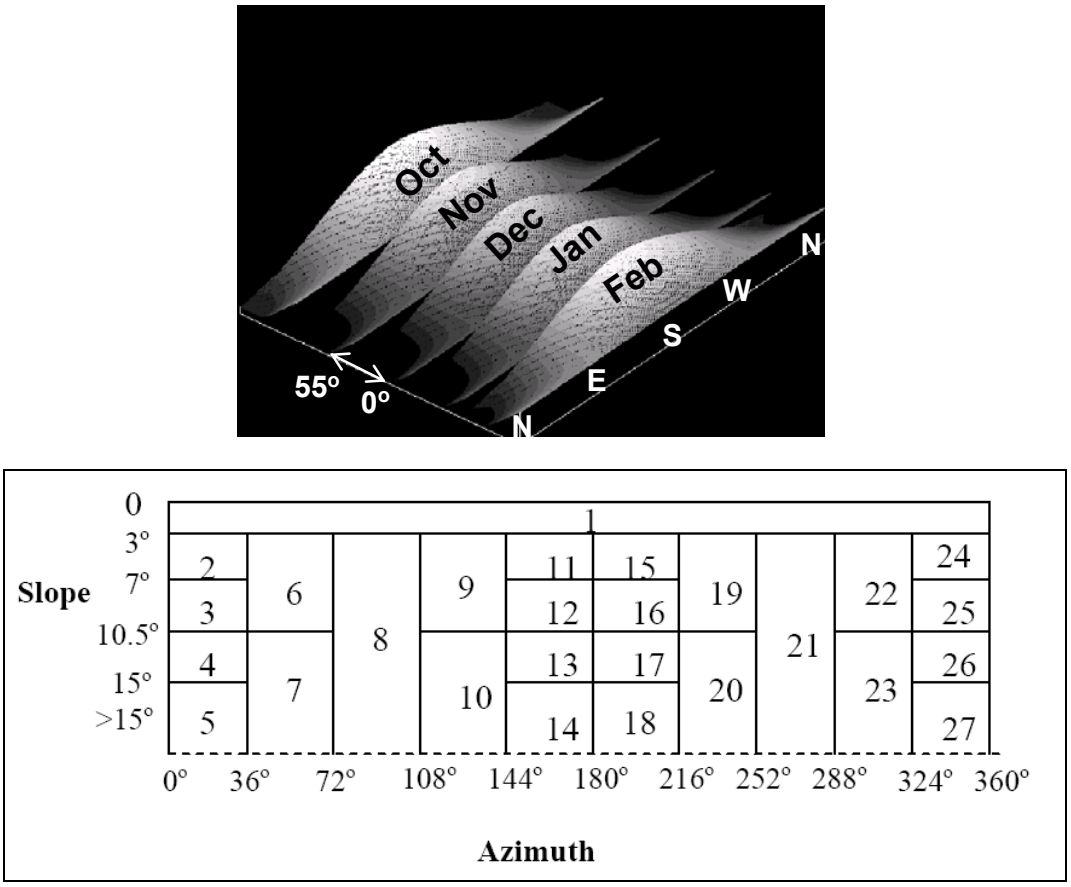

Figure 2. (Top) Relative clear sky radiation for the months of October through February plotted for terrain slopes of 0° to 55° for each month, and for all azimuths. (Bottom) SLTHERM solutions were obtained for the center points of these 27 slope–azimuth regions.

METHODS

Distributing the snowpack energy balance

Terrain elevation, slope, azimuth, and forest canopy greatly influence the mass and energy balance of the snowpack and the spatial distribution of snowpack properties. Our approach to distributing a mass and energy balance in the hilly, forested terrain of New England was to modify meteorological data measured at an open site so that it represents the meteorological gradients imposed by elevation, slope, azimuth, and forest cover. The energy balance of a snowpack may be expressed as

$$Q_M + Q_\Delta = Q_K + Q_L + Q_E + Q_H + Q_P + Q_G \quad (1)$$

where

Q_M = snowmelt,
$Q\Delta$ = change in stored heat,
Q_K = solar (or shortwave) radiation,
Q_L = terrestrial (or longwave) radiation,
Q_E = latent heat transfer (evaporation and condensation),

Q_H = sensible heat transfer,
Q_P = heat advected by rainwater, and
Q_G = conduction of ground heat.

South-facing slopes receive more solar radiation (Fig. 2). Forest canopies transmit only a percentage of the above canopy radiation to the snowpack; decrease longwave losses under cold, clear sky conditions; emit longwave radiation; and reduce wind speeds that reduce latent and sensible heat transfers. Precipitation and temperature lapse rates combine to accumulate more snow at higher elevations.

The meteorological data used were collected by the Forest Service at the Hubbard Brook Experimental Forest (HBEF) at 252-m elevation in an open field during the fall of 2002 and winter of 2003 (USDA 2004). Meteorological variations were created from the original base meteorology for 540 combinations of 27 slope–azimuths, four elevations (300, 500, 700, and 900 m) and five canopy solar transmissivities (0.14, 0.3, 0.5, 0.75, and 1.0). Canopy transmissivity (*Tr*) is a continuous variable rather than discrete; however, most forest cover maps are categorical and these discrete values were chosen to represent conifer, mixed conifer-deciduous, deciduous, sparse canopy, and no canopy, respectively.

Solar and terrestrial radiation

Solar radiation on slopes was calculated within SLTHERM using a cosine correction for illumination angle. Subcanopy shortwave radiation (K_{SC}) was calculated from solar radiation measured in the open (K_{IN}):

$$K_{SC} = K_{IN}\, Tr\,. \tag{2}$$

Reflected solar radiation was calculated using a constant albedo of 0.78:

$$K_{SCout} = 0.78\, K_{SC}\,. \tag{3}$$

Terrestrial radiation under the forest canopy ($L_{INforest}$) was calculated as

$$L_{INforest} = \left(1 - Tr\right) \varepsilon\, TempK^4 + \left(Tr\, L_{IN}\right) \tag{4}$$

where emissivity (ε) of the forest is taken as 0.96, the effective temperature of the forest is estimated by the air temperature (*TempK*), and σ is the Stephan–Boltzman constant (5.67×10^{-8} Wm^{-2} K^{-4}). L_{IN} is terrestrial radiation in the open (no canopy) and is calculated for three conditions: 100% clear ($L_{INclear}$), 100% cloudy ($L_{INcloud}$), and partly cloudy (L_{INpart}).

$$L_{INcloud} = \varepsilon\, \sigma\, TempK^4\,. \tag{5}$$

$$L_{INclear} = L_{INcloud} - A + OFF\,. \tag{6}$$

$$A = -0.4842\,[228 + 11.6\left(S_{VP}{}^{0.5} - A_{VP}{}^{0.5}\right)]\,. \tag{7}$$

$$L_{INpart} = L_{INcloud} - CI\,\left(A - OFF\right). \tag{8}$$

Equations 5, 6, and 7 were adapted from Anderson and Baker (1967) with a locality offset (*OFF*) determined for a site near Danville, Vermont (Melloh et al. 2004). S_{VP} and A_{VP} are saturation and actual vapor pressures. The clear-sky index (*CI*) is the ratio of observed solar radiation K_{IN} to clear-sky radiation K_{CS} calculated by methods presented by Dingman (1993).

Temperature, precipitation, windspeed

An average temperature lapse rate of –6.5 °C over 1000-m elevation rise was adopted. Precipitation gage undercatch was corrected in the base meteorology by adding between 0 to 41 percent of the measured precipitation over the windspeed range of 0 to greater than 7 ms^{-1} for a Universal gage with an Alter shield (Goodison 1978). A precipitation multiplier (*Pm*) applied with increased elevation (*E*)

$$P_M = 1 + \left(\frac{E - 252}{1000} \right) 0.75 \tag{9}$$

was adapted from Dingman's (1988, 1993) study of mean annual precipitation–elevation trends in New Hampshire and Vermont. Precipitation interception loss (P_I) was expressed in terms of canopy transmissivity (*Tr*) as

$$P_I = \left(1 - Tr\right) P_M \tag{10}$$

and P_I was limited to a maximum of

$$P_{\mathrm{Im}ax} = 0.0005 \left(1 - Tr\right)^3 . \tag{11}$$

Precipitation type was assumed to be rain if the temperature was above 275.5 K, snow below 273.2 K and a mix of snow and rain between these two temperatures (Jordan 1991). The initial snow-grain diameter was set at 0.0000254 m. The results of using Equations 9, 10, and 11 (Fig. 3) are increased precipitation (rain and snow) and increased snowfall with increased elevation. There is also decreased precipitation and snowfall under fuller canopies. The larger difference between the 300- and 500-m elevation snowfalls indicates a snowline occurs, at times, below the 500-m elevation (Fig. 3).

A wind lapse rate was set at 15% increase for each 200-m elevation gain. Wind modification by canopy was an adaptation of an equation suggested by Dunne and Leopold (1978)

$$W = w\left[1 - 0.8\left(1 - Tr\right)\right] \tag{12}$$

where *w* is wind measured in the open and *W* is wind in the subcanopy.

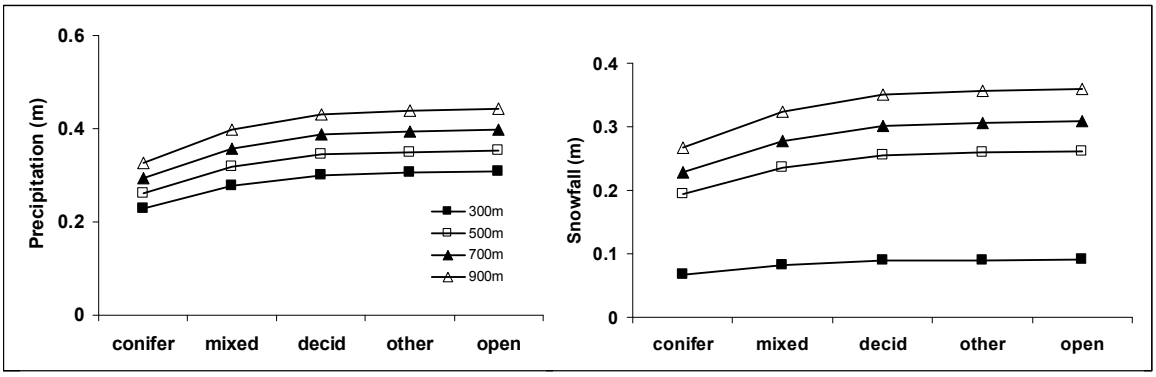

Figure 3. Precipitation and snowfall values are water equivalent summed over Julian days 300 to 110. (Left) Increased precipitation with elevation and increased interception with increased canopy fullness. (Right) Increased snowfall with elevation, increased interception with increased canopy fullness, and snowline development below 500 m. Only snowfalls for temperatures below 273.2 K are included.

SLTHERM Model initiation

Snowpack properties for the 540 meteorological sub-environments were modeled with SLTHERM. SLTHERM is a new version of SNTHERM (Jordan 1991) that has enhanced capability to model moisture and energy transfer between the snowpack and soil. SNTHERM is a well-tested and internationally known physically based snow process model. The simulation period initiated on 27 October (Julian day 300) and continued through snow accumulation and finally snowmelt. An initial snow temperature profile was available from Sleepers River Research Watershed (SRRW) at 900-m elevation and lapsed at a rate of 6.5 °C over 1000 m to the lower elevations.

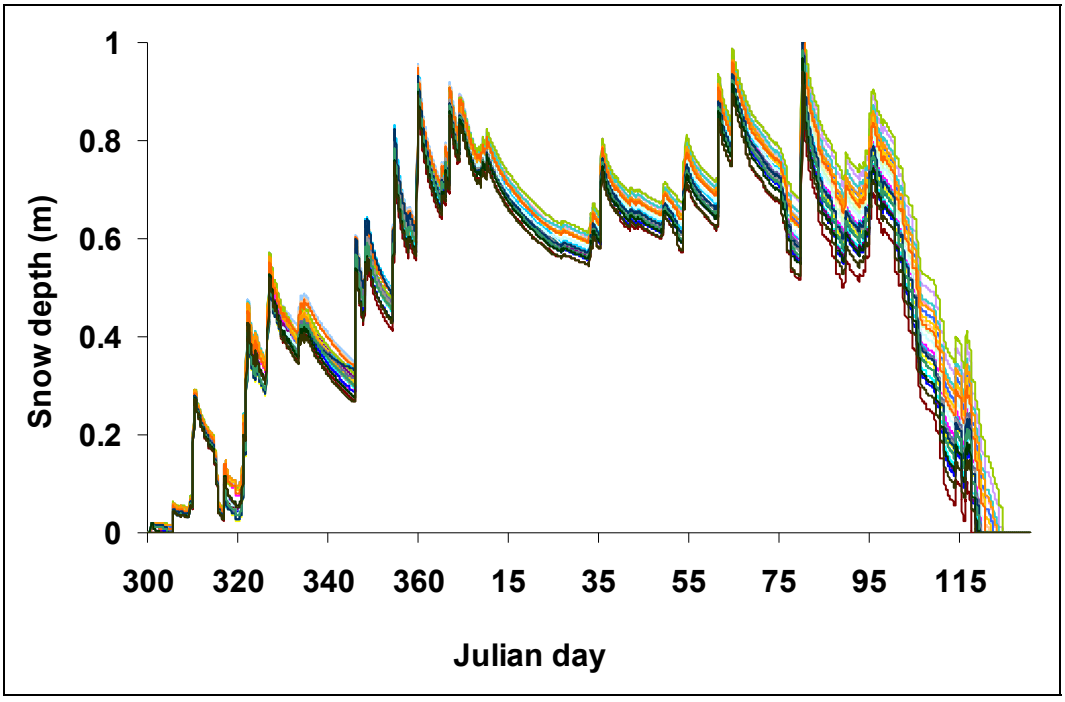

Figure 4. The modeled snow depth time-series for each of the 27 slope–azimuth cases for sparse forest. The top line is the most north-facing, and the bottom line the most south-facing modeled time series.

RESULTS

Shaped solution domains for snow depth

The snow model solutions (Fig. 4) for sparse canopy at 900-m elevation for each of the 27 slope–azimuth cases illustrate that the snow depths differentiate with time following snowfall events, and that the differentiation becomes more pronounced in late winter and spring as the snowpack ablates. The slope–azimuth and canopy dependence of solar radiation is the driving force behind snow property differentiation. On day 60 the snowpack has differentiated mildly with azimuth and terrain slope (Figs. 4, 5), by day 82 additional snow has fallen and further differentiation has occurred, and on day 110 the snowpack is shallow and highly differentiated. The 540 model solutions generated output for 20 time-series plots such as Figure 4, one for each of the five forest and four elevation combinations.

A three-dimensional (3-D) solution domain in the shape of a pinched cone is suggested by the terrain slope versus snow-depth plot (Fig. 5) if one visualizes the bold lines (east-facing azimuths) to be in the foreground and the dashed lines (west-facing azimuths) to be in the background. The cone vertex position along the x-axis (Fig. 5) represents the snow depth for the no-slope case and the vertex translates to the right along the x-axis in response to new snow (day 60 to day 82) or to

the left in response to snow compaction or ablation (day 82 to day 110). The increased radius of the cone indicates increased snow depth differentiation by slope–azimuth with increased terrain slope. Elongation along the north-south axis of the cone (Fig. 6) occurs because snow depth differentiates more for north- to south-facing (x-axis) than for east- to west-facing slopes (y-axis).

A pinched-cone shape that approximates the solution domain (Fig. 6) is given by the equation

$$z = \sqrt{\frac{x^2 + y^2}{a^2}} - \sqrt{\frac{x^2}{b^2}} \tag{13}$$

where x and y are Cartesian coordinates that determine the radius

$$r = \sqrt{x^2 + y^2} \tag{14}$$

and where the radius represents the difference in the snow depth from the 0° terrain slope case. The slope azimuth (θ) direction is given by a radial coordinate system about the *z*-axis (Fig. 6). Coefficients *a* and *b* satisfy the equations

$$a = \frac{|y|}{z} \qquad \text{when } x = 0 \text{ and y = minimum radius} \tag{15}$$

$$b = \left(\frac{1}{a} - \frac{z}{|x|} \right)^{-1} \qquad \text{when } y = 0 \text{ and x= maximum radius.} \tag{16}$$

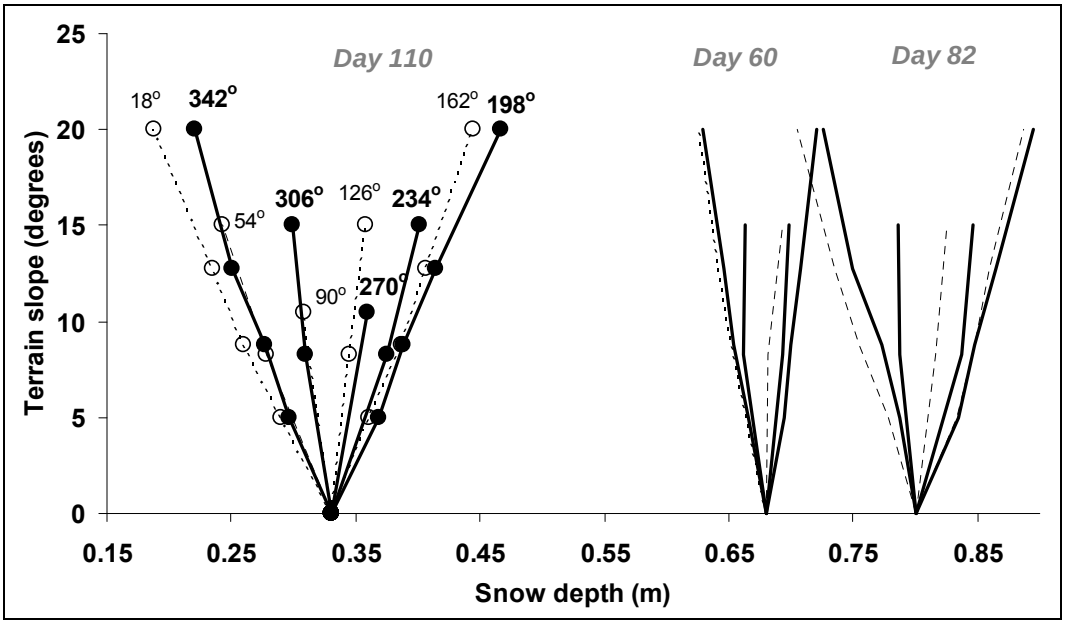

Figure 5. Modeled snow depths (x-axis) for days 60, 82, and 110 plotted against terrain slope. The circles on day 110 indicate the snow model solutions. Bold lines are east-facing azimuths and dashed lines are west-facing azimuths. The 18° azimuth is the most south-facing and 198° the most north-facing.

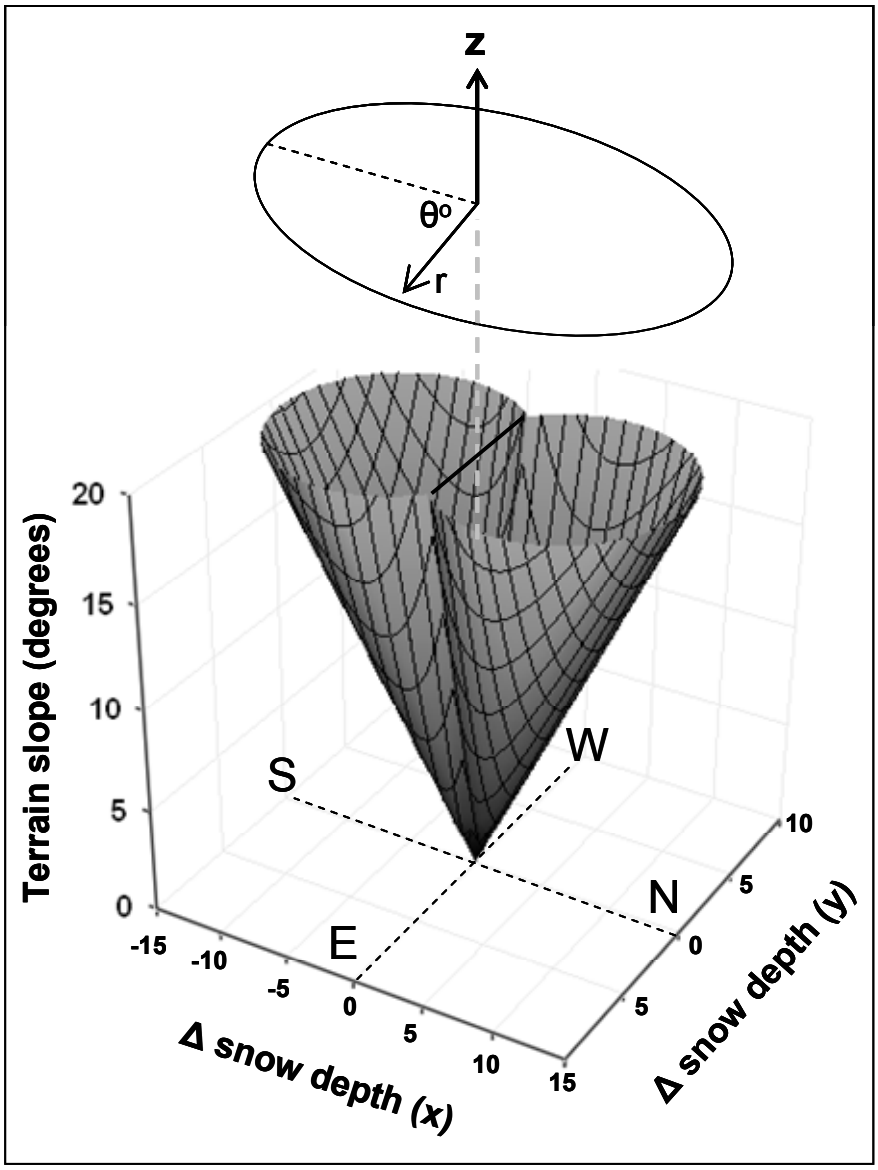

Figure6. The squashed-cone shaped solution in Cartesian and cylindrical coordinate systems, representing the snow-depth differentiation with slope and azimuth.

The SLTHERM model solutions plot along the z = 8.5° and z = 20° contours (Fig. 7) of the pinched cone and verify that equation 13 approximates the shape of the solution domain. South-facing Δ snow depths are negative and north-facing Δ snow depths are positive (Fig. 6 and 7) and, as a result, the shape given by equation 13 must be corrected to pass through r = 0 on the minimum axis. The available SLTHERM solutions suggest that an 18° rotation corrects for east-west asymmetry. The long axis is along 18° and 198° rather than directly north-south and the minimum axis is along 108° and 288° azimuths (rather than directly east-west). The asymmetry likely arises because west-facing slopes receive the afternoon sun through a more transmissive atmosphere than east-facing slopes that receive the morning sun. A gradual correction to r=0 at the 108° and 288° azimuths modifies the cone shape within ±18° of the minimum axis (between 90° and 126°, and between 270° and 306°) where SLTHERM solutions were not computed (Fig. 7).

Pinched-cone dimensions for each slope–azimuth–forest environment were determined by finding the coefficients (*a* and *b*) needed to match the SLTHERM solutions for each respective environment. Some of the SLTHERM model solutions do not lie as close to the contours as others (Fig. 7). Additional model studies at additional azimuths are needed to refine the rotation and fundamental shape if necessary, and shorter time steps (< 1hr) may be necessary to obtain more consistent results. Equation 13 (with the r=0 at the minimum axis correction) is a reasonable first approximation of the solution domain shape. An equation that predicts *r* (Δ snow depth) as a function of *z* and θ^o will be developed for future applications (Melloh et al. in review).

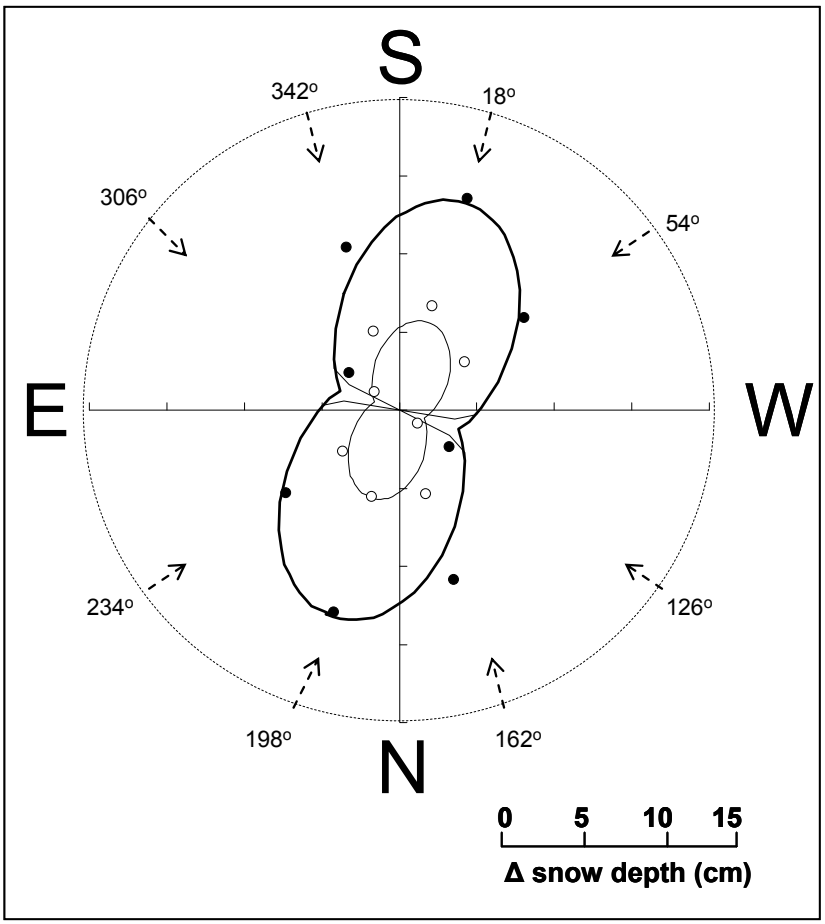

Figure 7. Contour plot of the cone at terrain slopes of z = 20° (outer contour) and 8.5° (inner contour) with day 110 sparse forest SLTHERM solutions (circles) shown. Solid circles are for z = 20° and open circles for z = 8.5° terrain slopes. The facing azimuths are indicated on the compass. The Δ snow depths (cm) are positive beneath and negative above the east-west axis. An r=0 correction is sketched in at the minimum axis.

Shaped solution transitions over time and canopy gradients

The shaped solutions for deciduous forest for days 60, 82, and 110 (Fig. 8 top) present an expanding cone over time as the snowpack ablates. The radii of the cone-shaped solutions contract progressively across the decreasing canopy transmittance gradient of open to conifer (Fig. 8 bottom). The cone-shaped solutions over the canopy transition nest neatly inside one another when the vertices are co-located.

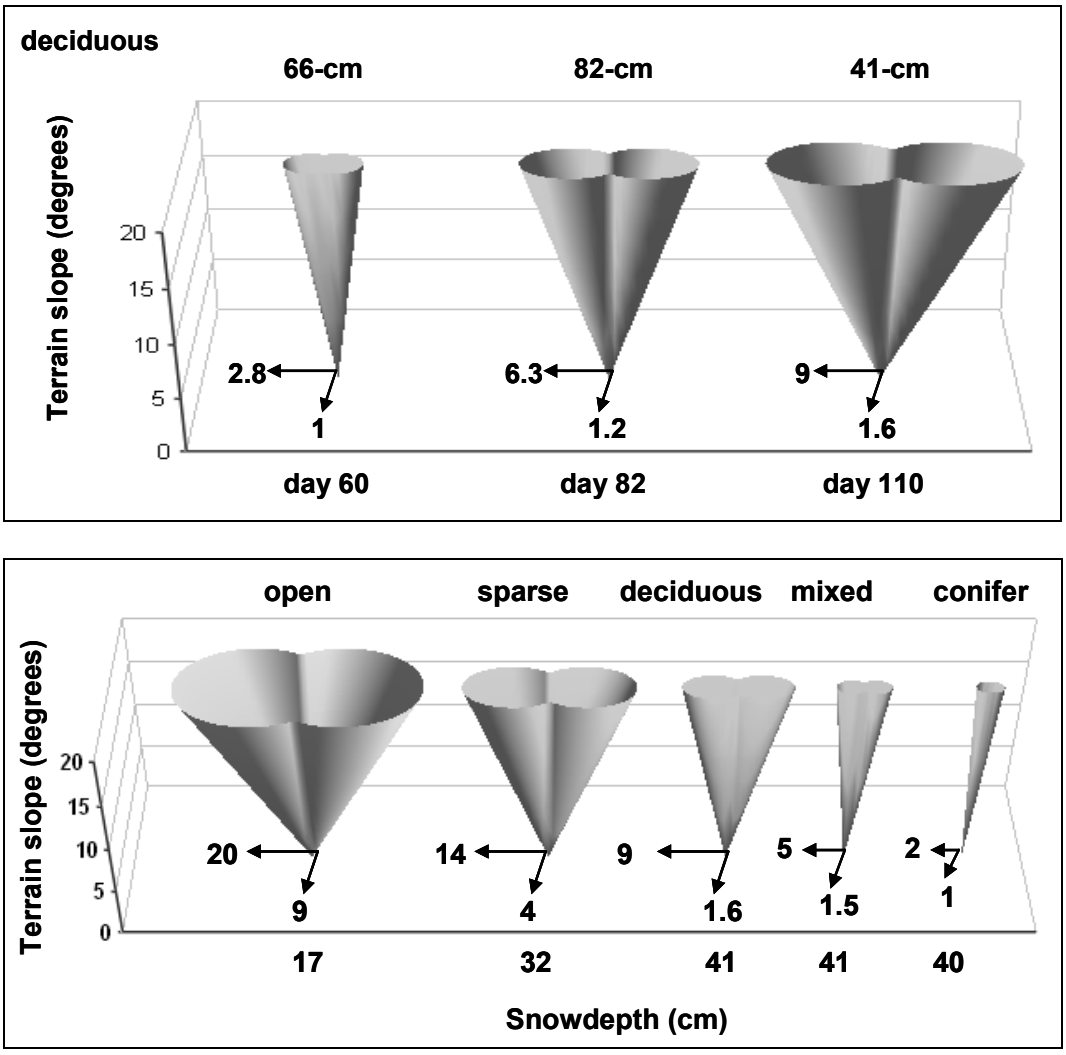

Figure 8. (Top) Snow depth shaped solutions over time in the deciduous forest at 900-m elevation. The snow depths for 0° terrain slopes are shown above each cone for days 60, 82, and 110. In both top and bottom, the arrows at the vertices represent the maximum (north-south) and minimum (east-west) Δ snow depths (cm) relative to the 0° slope case. (Bottom) Snow depth shaped solutions over the forest environmental range on day 110 at 900-m elevation. Snow depths for 0° slopes are listed on the x-axis. Corrections on minimum axes not shown.

Shaped solutions for snow water equivalent and density

Snow water equivalent (SWE) variation with terrain slope and azimuth (Fig. 9) displays similarly to snow depth variation (Fig. 5). The SWE solution domain can also be approximated by the pinched-cone equation (Fig. 10). A snow density shaped solution was calculated by dividing the axes dimensions of the snow water equivalent cone by those of the snow depth cone (Fig. 10).

DISCUSSION

Shaped solution domains for snow properties are a way to extend what we know about snow property differentiation with solar radiation and forest cover. The snow cone is an interpolation surface; a few model runs or measurements are exploited to define a continuous solution. The pinched-cone shape can be defined by three model runs: 1) the no-slope case, 2) a slope–azimuth combination that defines the maximum diameter of the cone, and 3) a slope–azimuth combination

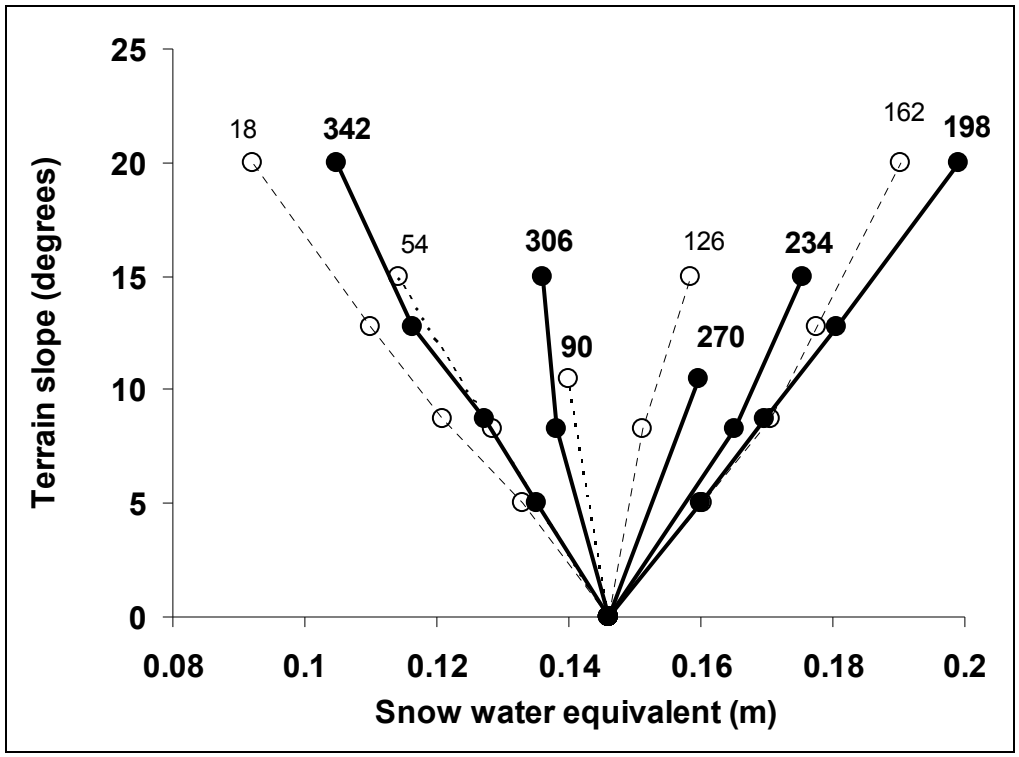

Figure 9. Modeled snow water equivalent (x-axis) for day 110 plotted against terrain slope. The circles indicate the SLTHERM solution points.

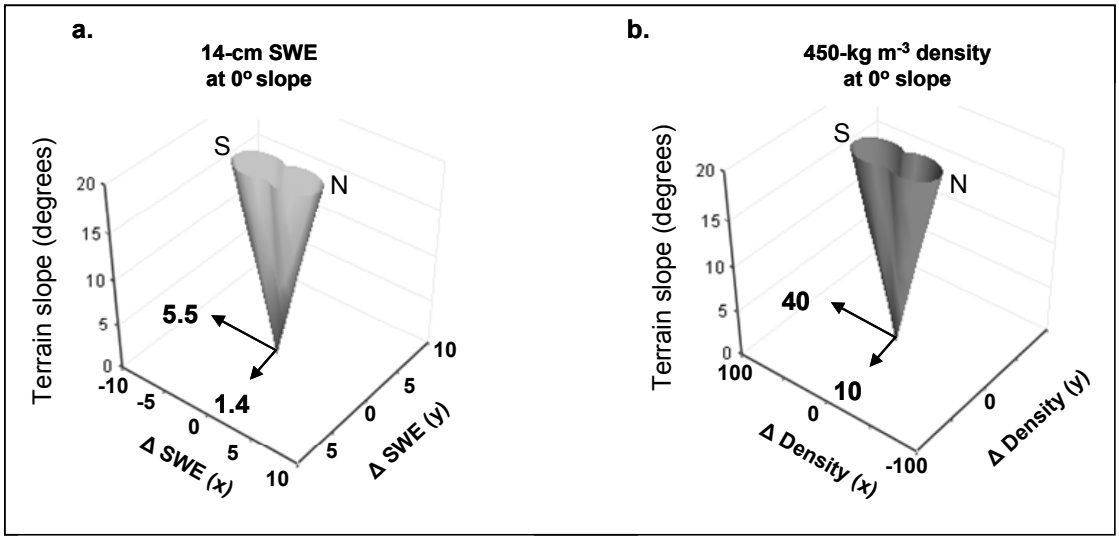

Figure 10. (Left) Shaped solution for snow water equivalent for day 110 in the sparse forest at 900-m elevation. (Right) Shaped solution for snow density derived from the depth and water equivalent cones. The arrows at the vertices represent the maximum (north-south) and minimum (east-west) Δ SWE (cm) and Δ density (kg m^{-3}), respectively, relative to the 0° slope case. The arrows are not to scale. Corrections to r=0 on minimum axes are not shown.

that defines a second point on the cone. The three points defining the shaped solution do not have to be these specific ordinates because any three points on the cone will define the shape; however, points near these extremes are recommended. The fundamental shape of the solution domain can be used to help plan snow measurement networks. In the absence of model solutions, measurements at a few key locations in a basin might be used to define a cone shape and provide an estimate of the snow properties for any slope–azimuth combination of similar canopy and elevation. Locations in contrasting canopy or elevation can define the change in cone dimension with these environmental gradients.

Mathematics on the solution domains provides another interpolation route. Our first application of the shaped solution domains will be to distribute snow depth and density across the landscape of the Ethan Allen Firing Range near Jericho, Vermont, for a vehicle mobility model. Interpolating between the shaped solution domains of the 20 slope–azimuth–canopy–elevation environments permits creation of a continuous snow property map across the landscape if continuous maps of each of the environmental variables are available (slope, azimuth, canopy transmissivity, and elevation). The forest map at Ethan Allen Firing Range is categorical, thus our forest component interpolation will also be categorical. Other examples of solution domain mathematics include snow density computations from snow water equivalent and snow depth cones, and melt rate calculations by differencing snow water equivalent cones over time. Equation 13 (with a shape correction to r=0 at the minimum axis) is a good approximation of the fundamental shape for our intended application. Additional model studies at shorter time steps to improve model consistency and potentially refine the azimuths of the major axes are warranted. An equation that predicts r (Δ snow depth) as a function of z and θ^o will be developed for future applications (Melloh et al. in review).

The shaped solution domains were developed to map snow properties in a hilly forested terrain typical of New Hampshire and Vermont and over a relatively small basin. The method is likely to be useful in other situations, though adaptations are needed to deal with large basins, topographic shading, and blowing snow. The presented method will not be especially useful on plains and prairies where the topography is flat, and where there is significant blowing snow. Using a cone method over larger basins will require adaptations to account for latitudinal and longitudinal meteorological gradients. The cone does not account for topographic shading, an important consideration in mountainous basins. Also of interest is how the cone shape changes with changing maximum sun angle at lower and higher latitudes. It is also important to recognize that the cone solutions represent mean snow properties, and on any given slope in the field there will be variability about the mean due to microclimate and local deposition.

CONCLUSION

A shaped solution domain was identified for snow depth, water equivalent, and density. The pinched-cone shape describes the differentiation of the snow properties with slope and azimuth relative to the no-slope case represented by the vertex of the cone. The shaped solution domain is approximated by an analytical equation with only two coefficients. A time series of snow properties over a snow season can be described efficiently by a time series of three numbers: the snow property for the no-slope case, and the two coefficients. Interpolating between the shaped solution domains of slope–azimuth–canopy–elevation environments permits creation of a continuous snow property map across the landscape if continuous maps of each of the environmental variables are available (slope, azimuth, canopy transmissivity, and elevation). Knowledge of the shape of the solution domain can be exploited to portray snow property differentiation across environments and may lead to less model-intensive approaches of estimating snow properties across a landscape.

ACKNOWLEDGEMENTS

This work was funded by the U.S. Army AT42 High-Fidelity Ground Platform and Terrain Mechanics Modeling Program. The meteorological data used in this publication were obtained by scientists of the Hubbard Brook Ecosystem Study; this publication has not been reviewed by those scientists. The Hubbard Brook Experimental Forest is operated and maintained by the Northeastern Forest Experiment Station, U.S. Department of Agriculture, Radnor, Pennsylvania. We thank Susan Frankenstein and Paul Richmond for their reviews of this manuscript.

REFERENCES

Anderson EA, Baker DR. 1967. Estimating incident terrestrial radiation under all atmospheric conditions. *Water Resources Research* **3**(4): 975–988.

Dingman SL. 1988. Application of kriging to estimating mean annual precipitation in a region of orographic influence. *Water Resources Bulletin* **24**(2): 329–339.

Dingman SL. 1993. *Physical Hydrology*. Englewood Cliffs, NJ: Prentice Hall, 575 pp.

Dunne T, Leopold LB. 1978. *Water in Environmental Planning*. San Francisco, CA: W.H. Freeman and Co.

Flerchinger GN, Cooley KR, Deng Y. 1994. Impacts of spatially and temporally varying snowmelt on subsurface flow in a mountainous watershed: 1. Snowmelt simulation. *Hydrological Sciences* **39**(5): 507–520.

Goodison BE. 1978. Accuracy of Canadian snow gage measurements. *Journal of Applied Meteorology* **27**: 1542–1548.

Jordan R. 1991. A one-dimensional temperature model for a snow cover: Technical documentation for SNTHERM.89. U.S. Army Cold Regions Research and Engineering Laboratory, Special Report 91-16.

Marks D, Domingo J, Susong D, Link T, Garen D. 1999. A spatially distributed energy balance snowmelt model for application in mountain basins. *Hydrological Processes* **13**: 1925–1959.

Melloh RA, Richmond P, Shoop S, Coutermarsh B, Affleck R. in review. Continuous snow property mapping for mobility models. *Cold Regions Science and Technology*.

Melloh RA, Hall TJ, Bailey RN. 2004. Radiation data corrections for snow-covered sensors: Are they needed for snowmelt modeling? *Hydrological Processes* **18**: 1113–1126.

Richmond, P., Reid A, Shoop S, Mason G. 2005. Terrain Surface Codes for an All-Season, Off-Road Ride Motion Simulator, MSIAC *M&S Journal* On-Line.

Shoop S, Coutermarsh B, Reid A. 2004. All-Season Virtual Test Site for a Real-Time Vehicle Simulator, Paper No. 2004-01-2644, *SAE Transactions* **113**(2): 333–343.

Tarboton DG, Luce CH. 1996. *Utah Energy Balance Snow Accumulation and Melt Model (UEB) Computer Model Technical Description and Users Guide.* Utah Water Research Laboratory and USDA Forest Service Intermountain Research Station: 64 p.

U.S. Department of Agriculture, Forest Service, Northeastern Research Station, Hubbard Brook. 2003. Web page (http://www.hubbardbrook.org), GIS coverages, and overview (guidebook).